

3 4456 0513467 2

NATIONAL LABORATORY

operated by

UNION CARBIDE CORPORATION

NUCLEAR DIVISION

for the

U.S. ATOMIC ENERGY COMMISSION



ORNL - TM - 2019

1

EFFECTS OF IRRADIATION ON DUCTILITY

J.O. Stiegler and J.R. Weir, Jr.

OAK RIDGE NATIONAL
CENTRAL RESEARCH
DOCUMENT COLLECTION
LIBRARY LOAN
DO NOT TRANSFER TO ANOTHER
If you wish someone else to use
document, send in name and address
and the library will arrange to loan it.

UCN-7969
13 3-67

NOTICE This document contains information of a preliminary nature and was prepared primarily for internal use at the Oak Ridge National Laboratory. It is subject to revision or correction and therefore does not represent a final report.

LEGAL NOTICE

This report was prepared as an account of Government sponsored work. Neither the United States, nor the Commission, nor any person acting on behalf of the Commission:

- A. Makes any warranty or representation, expressed or implied, with respect to the accuracy, completeness, or usefulness of the information contained in this report, or that the use of any information, apparatus, method, or process disclosed in this report may not infringe privately owned rights; or
- B. Assumes any liabilities with respect to the use of, or for damages resulting from the use of any information, apparatus, method, or process disclosed in this report.

As used in the above, "person acting on behalf of the Commission" includes any employee or contractor of the Commission, or employee of such contractor, to the extent that such employee or contractor of the Commission, or employee of such contractor prepares, disseminates, or provides access to, any information pursuant to his employment or contract with the Commission, or his employment with such contractor.

Contract No. W-7405-eng-26

METALS AND CERAMICS DIVISION

EFFECTS OF IRRADIATION ON DUCTILITY

J. O. Stiegler and J. R. Weir, Jr.

Paper presented at the ASM Weekend Seminar on Ductility,
October 14-15, 1967, Cleveland, Ohio. To be published
by the American Society for Metals.

JANUARY 1968

OAK RIDGE NATIONAL LABORATORY
Oak Ridge, Tennessee
operated by
UNION CARBIDE CORPORATION
for the
U.S. ATOMIC ENERGY COMMISSION

LOCKHEED MARTIN ENERGY RESEARCH LIBRARIES



3 4456 0513467 2

CONTENTS

	Page
Abstract	1
Introduction	1
Considerations of Plastic Deformation and Fracture	4
Low-Temperature Characteristics — Work Hardening	4
High-Temperature Characteristics — Grain-Boundary Fracture	7
Structural Effects of Irradiation	9
Concepts	10
Observations of Irradiated Materials	16
Plastic Flow and Fracture in Irradiated Materials	26
Dislocation-Defect Interactions	26
Ductility and Mechanical Properties Effects at Low Temperatures	29
Ductility at High Temperatures	35
Behavior of Gases, Bubbles, and Grain Boundaries	38
Concluding Remarks	43
Acknowledgments	44
References	45

EFFECTS OF IRRADIATION ON DUCTILITY

J. O. Stiegler and J. R. Weir, Jr.

ABSTRACT

The effect of neutron irradiation on the ductility of metals is of great technological interest because of their utilization in nuclear power reactors. The problem of reduced ductility resulting from irradiation is divided into two parts: a low-temperature region in which plastic instability limits elongation and a high-temperature problem in which grain-boundary cracks cause failure. Fracture occurs by the same processes in unirradiated materials, the effect of irradiation being to reduce the strain at which failure occurs. In this report the general aspects of deformation and fracture at high and low temperatures are discussed. An introduction is given to the concepts involved in neutron irradiation and to changes in the lattice introduced by irradiation. These are illustrated by electron micrographs of irradiated materials. Changes in mechanical properties as a result of irradiation are described and explained in terms of the corresponding microstructural changes.

INTRODUCTION

The nuclear power reactors currently under development by the Atomic Energy Commission are potentially more economic in their electrical power production costs than the reactors presently being constructed by the utility companies. These reactors of the future will require higher performance of the materials of construction than today's reactors. One of the more important properties of the alloys being used and those under consideration is their ability to deform small amounts while in service at high temperatures to accommodate thermal stresses and those stresses imposed by the fissioning fuel.

The quantitative measure of the ability of a metal to deform without fracturing may be defined as the ductility of the metal. As may be observed in the other chapters in this book, there are numerous measures of ductility, defined in various ways, and having as their bases a variety of types of tests and testing conditions. Because of our rather poor understanding of the microscopic aspects of fracture in metals, it has been necessary to develop tests representative of the deformations and stress systems operating on the material to assess its behavior under the service conditions. The service conditions may be those encountered during fabrication of the material into the desired shape or during use of the material in a structure.

We shall restrict our discussion to the behavior of metals used in those parts of a nuclear reactor system that are exposed to the high temperature and the neutrons emanating from the fissioning fuel. This chapter will also consider only those metals that are normally considered ductile; that is, not subject to brittle fracture (cleavage) in the classical sense. The effect of radiation damage on the brittle fracture of pressure vessel steels has been reviewed recently by others (1,2).

No single set of symptoms characterizes radiation-induced embrittlement. Rather, the behavior is a sensitive function of both the irradiation and deformation temperatures, as can be seen in Table 1. Low-temperature irradiation followed by low-temperature deformation results in a large increase in yield stress accompanied by a large decrease in true uniform strain, while no effect is observed in mechanical properties at low test temperatures if the irradiation temperature is high. On the other hand, a high-temperature test following either high- or low-

Table 1. Effect of Irradiation on the Mechanical Properties of
Stainless Steels as a Function of Deformation and
Irradiation Temperature^a

Mechanical Properties	Deformation Temperature ^b		
	T < 1/2 T _m		T > 1/2 T _m
	Low Irradiation Temperature	High Irradiation Temperature	Low and High Irradi- ation Temperatures
Yield stress	large increase	no effect	no effect
Engineering ultimate stress	small increase	no effect	small decrease
True tensile stress	no effect	no effect	small decrease
True fracture stress	no effect	no effect	small decrease
True uniform strain	large decrease	no effect	decrease
True fracture strain	no effect	no effect	large decrease
Work hardening coefficient	large decrease	no effect	no effect

^aW. R. Martin and J. R. Weir, Jr., Effect of Irradiation Temperature on the Post-Irradiation Stress-Strain Behavior of Stainless Steel, Flow and Fracture of Metals and Alloys in Nuclear Environments Spec. Tech. Pub. No. 380, American Society for Testing and Materials, Philadelphia, Pa. 1965, p. 251.

^bT_m = absolute melting point of the alloy.

temperature irradiation shows no significant strength changes but a large decrease in true fracture strain. On this basis we will divide the problem of irradiation embrittlement into two parts, one associated with low irradiation and test temperatures and the other with high test temperatures. We will first consider general aspects of deformation at low and high temperatures and then discuss changes in microstructure brought about by irradiation. We will then examine the radiation-induced changes in mechanical properties and relate them to the corresponding microstructural changes.

CONSIDERATIONS OF PLASTIC DEFORMATION AND FRACTURE

The ductility in tension of materials that do not fracture by cleavage is limited by a plastic instability that results in local "necking" and shear fracture of the specimen at low temperatures or by intergranular fracture at high temperatures. Let us briefly consider each of these processes.

Low-Temperature Characteristics - Work Hardening

Plastic deformation of metals in tension usually results in a plastic instability or local necking after some amount of strain. This local necking limits the elongation of the material. It is important to understand the conditions under which this instability occurs, since it is related to our definition of ductility. Examination of the engineering stress (σ)-strain (ϵ) curve in Fig. 1 reveals that the plastic instability occurs when the engineering stress is a maximum. At this point

$$\frac{d\sigma}{d\epsilon} = 0 , \quad (1)$$

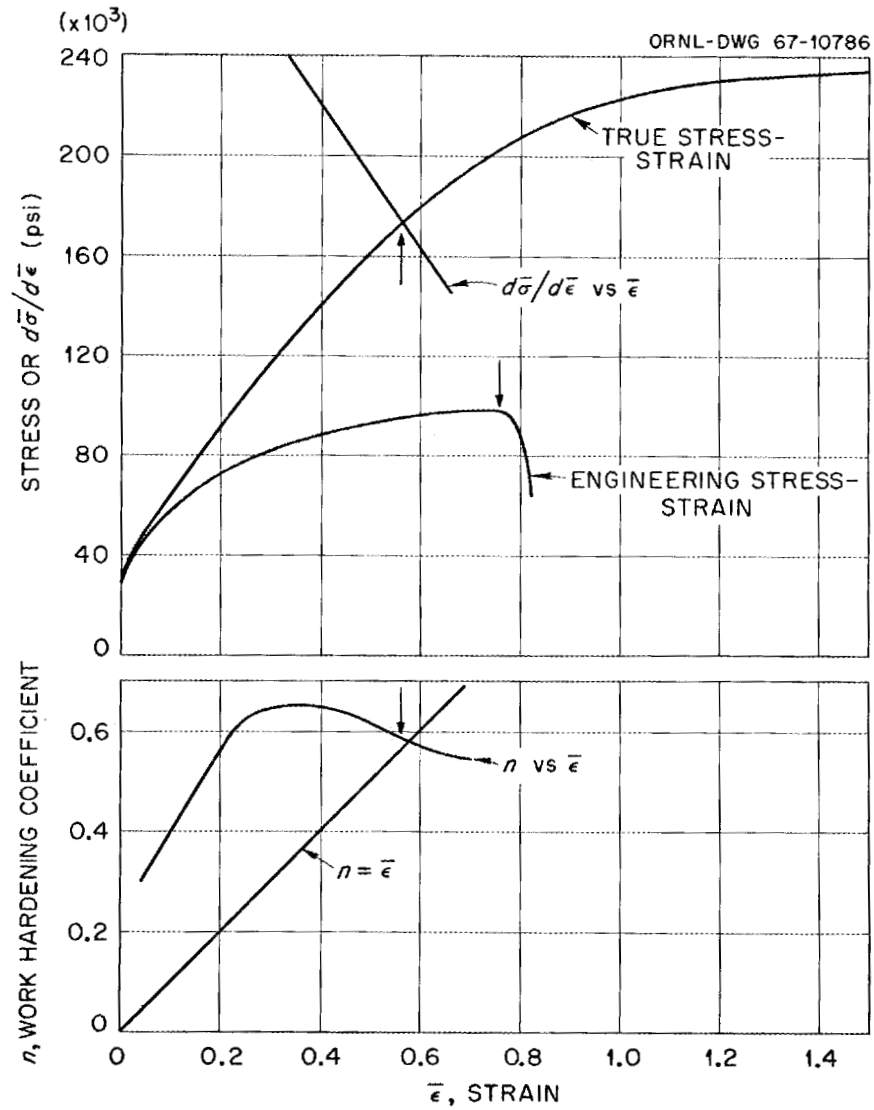


Fig. 1. The Stress-Strain Characteristics of Type 304 Stainless Steel at Room Temperature. The arrows indicate the strain at which the plastic instability was observed to develop.

where

σ = the engineering stress (the load, L , divided by the initial cross-sectional area of the specimen, A_0),

ϵ = the strain $(\frac{l - l_0}{l_0})$,

l = length of sample,

l_0 = the initial length of the sample.

With this and the definition of σ ,

$$dL = 0 . \quad (2)$$

From the definition of true stress $\bar{\sigma}$, we may obtain

$$L = \bar{\sigma} A , \quad (3)$$

where

A = cross-sectional area, and by differentiating

$$dL = \bar{\sigma} dA + A d\bar{\sigma} = 0 . \quad (4)$$

The constant volume assumption allows us to write

$$A_0 l_0 = A l . \quad (5)$$

This, with the definition of strain above, may be rearranged to yield

$$A_0 = A(1 + \epsilon) . \quad (6)$$

Differentiating, we obtain

$$0 = A d\epsilon + (1 + \epsilon) dA . \quad (7)$$

Substituting Eq. (7) appropriately into Eq. (4),

$$d\bar{\sigma} = \bar{\sigma} \frac{d\epsilon}{1 + \epsilon} . \quad (8)$$

Since

$$d\bar{\epsilon} = \frac{d\epsilon}{1 + \epsilon} , \quad (9)$$

where

$\bar{\epsilon}$ = true or logarithmic strain,

then, at the point of instability

$$\frac{d\bar{\sigma}}{d\bar{\epsilon}} = \bar{\sigma} . \quad (10)$$

If we assume a power-law relationship between true stress and strain, the work-hardening exponent

$$n = \frac{d \ln \bar{\sigma}}{d \ln \bar{\epsilon}} = \frac{\bar{\epsilon}}{\bar{\sigma}} \frac{d\bar{\sigma}}{d\bar{\epsilon}} . \quad (11)$$

This with Eq. (10) yields at the point of instability

$$n = \bar{\epsilon} . \quad (12)$$

Examination of Fig. 1 shows that Eqs. (10) and (12) are reasonably well obeyed for type 304 stainless steel.

High-Temperature Characteristics - Grain-Boundary Fracture

At high temperatures the condition of instability must involve the strain-rate dependence of the flow stress in addition to the rate independent considerations discussed above. An excellent review of the phenomenological theory including strain-rate effects has been recently

presented by Hart (3). We shall not discuss these principles here because the deformation at high temperatures of alloys of importance (as concerns irradiation effects on ductility) is generally terminated by intergranular fracture. This type of fracture illustrating no significant tendency for necking is shown in Fig. 2.

Mechanisms by which grain-boundary cracks are nucleated and grow at elevated temperatures are not well understood, although several qualitative concepts have been developed (4,5,6,7,8). The appearance of the cracks depends on the test temperature and stress; at lower temperatures and higher stresses the cracks have a characteristic wedge shape and

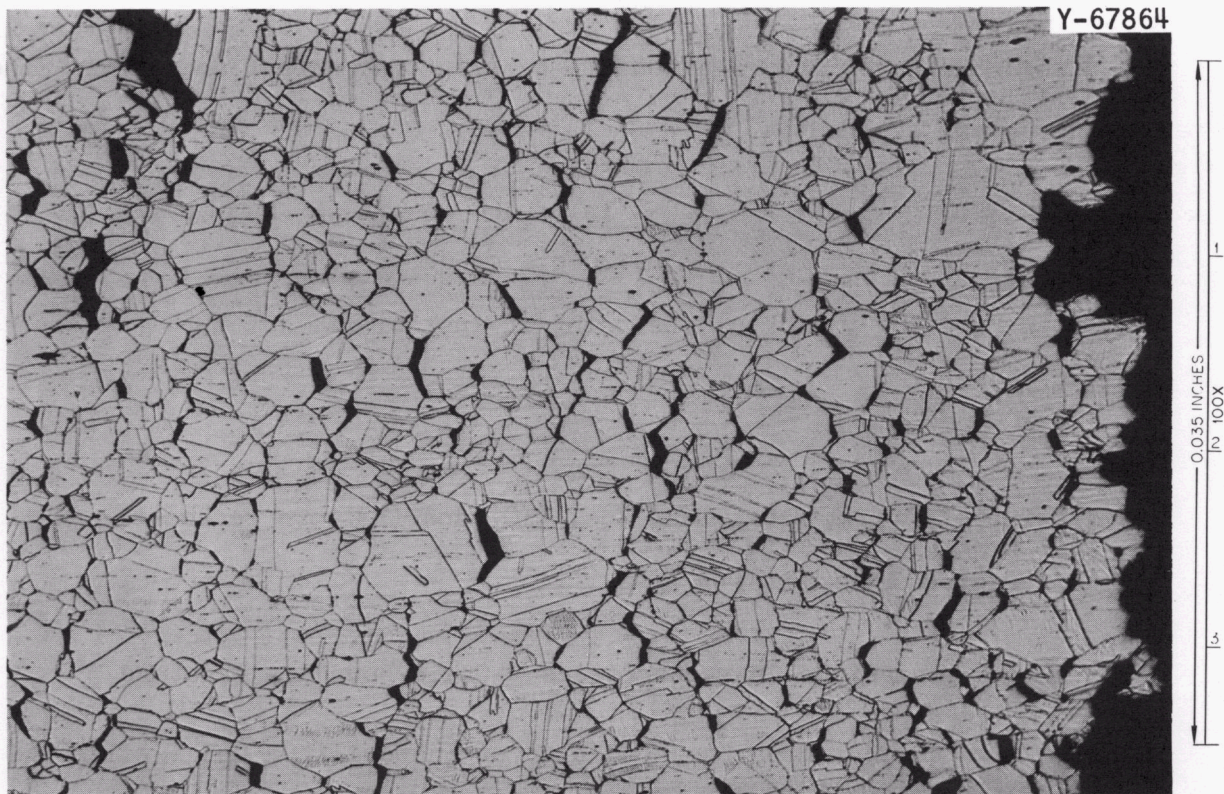


Fig. 2. Photomicrograph Showing the Characteristics of High-Temperature Fracture in Type 304 Stainless Steel. The stress was applied in the horizontal direction. Note the high density of intergranular cracks having the characteristic wedge appearance located below the fracture surface.

appear to emanate from triple grain junctions, giving the illusion that they are nucleated there. On the other hand, at higher temperatures and lower stresses rounded cavities appear on the grain-boundary surfaces and then grow and merge to form cracks. The view has been put forth that grain-boundary sliding blocked at triple grain junctions produces at the junctions tensile stress concentrations that ultimately exceed the strength of the solid and open a small crack. The wedge-shaped crack may then grow along the boundary by continued sliding, dislocation motion within the grains, or stress-induced diffusion of vacancies toward the tip of the crack. The voids on the grain-boundary surfaces are believed to be formed at ledges, jogs, or nonwetting particles in the boundary, which are opened by sliding. Growth may again occur by mechanical processes or vacancy condensation, although surface diffusion must occur sufficiently rapidly to allow the cavities to maintain nearly spherical shapes. As the cavities grow and merge, they form cracks, but scalloped edges reveal their origin.

STRUCTURAL EFFECTS OF IRRADIATION

The exposure of metals to high-energy neutrons and charged particles produces defects such as vacant lattice sites, interstitial atoms, and transmuted atoms (atoms having a different atomic number than the original). The charged particles normally produced in accelerators or by decay of radioactive isotopes travel only very short distances in metals (a few tens of microns at most). Thus, in a practical sense, their effects on ductility are difficult to assess experimentally and are perhaps only of scientific interest. However, energetic neutrons penetrate large distances into metals and can upon collision transfer sufficient energy to

the atoms of metals to dislodge them from their normal positions in the lattice. When a high-energy neutron hits the nucleus of an atom it also may introduce sufficient energy into the nucleus to transmute it to an atom of another chemical species with the emission of a charged particle. We shall discuss in the following the theory of these events in a qualitative way and then describe some observations of the structural damage in metals produced by neutron irradiation.

Concepts

Neutrons with energies between about 0.1 and 10 Mev are produced by the fission process. In a "thermal" reactor some of these are slowed down to thermal energy (i.e., approx 0.025 ev). The first consideration is to calculate the number of neutrons striking the material in the reactor. Since the neutrons are not monoenergetic, we are sometimes interested in the integral flux or the total number of neutrons of all energies

$$\phi = \int_0^{\infty} \phi(E) dE \quad (\text{neutrons cm}^{-2} \text{ sec}^{-1}) . \quad (13)$$

The time-integrated flux or total exposure (sometimes termed fluence) is

$$\int_0^t \phi(t) dt \quad (\text{neutrons cm}^{-2}) . \quad (14)$$

This is, of course, ϕt if the flux is constant with time.

The next quantity of interest is the number of interactions between the neutrons and the atoms in the metal. This is

$$N_r/N_o = \int \phi(E) \sigma(E) dE , \quad (15)$$

or for a monoenergetic flux of neutrons

$$N_r/N_o = \phi\sigma , \quad (16)$$

where

N_r/N_o = fractional number of interactions per second,

ϕ = neutron flux (neutrons $\text{cm}^{-2} \text{sec}^{-1}$),

σ = the microscopic cross section, a measure of the probability per neutron of an interaction (cubic centimeter).

Collisions between neutrons and lattice atoms may be treated in terms of elastic collisions between hard spheres. In this case the maximum energy transferred when a particle of mass m_1 and energy E_1 strikes a particle of mass m_2 at rest is

$$E_{\text{max}} = \frac{4m_1m_2}{(m_1 + m_2)^2} E_1 . \quad (17)$$

Since the neutron has a mass number of 1, this becomes

$$E_{\text{max}} \approx 4E_1/m_2 , \quad (18)$$

where m_2 is now the mass number of the struck particle. The average energy transfer is half the maximum amount. Now, if the energy transfer to the struck atom exceeds some threshold value, usually estimated to be about 25 ev, the atom will be displaced from its lattice site. Such an atom, termed a primary knock-on, will interact with lattice atoms in its vicinity, possibly displace some of them, and gradually come to rest. If the struck atom receives a large amount of energy, its more loosely bound electrons will be stripped from it leaving it highly ionized. Under these conditions it will lose energy primarily through electronic interactions, but as it slows down it will make frequent collisions with lattice atoms, the frequency increasing as the energy of the knock-on decreases.

A calculation of the total number of displaced atoms produced is obviously a complex problem. To illustrate the order of magnitude of the number we will follow the treatment of Kinchin and Pease (9). They assume that the knock-on loses energy entirely by ionization above some cutoff energy approximately equal to the mass number of the struck atom in kilo-electron volts.

The number of additional displaced atoms produced per primary knock-on atom is approximately

$$N_d = \frac{E}{2E_d} \text{ for } 2E_d < E < E_i, \quad (19)$$

and

$$N_d = \frac{E_i}{2E_d} \text{ for } E > E_i, \quad (20)$$

where

E = the energy of the primary knock-on,

E_d = the threshold displacement energy, approximately 25 ev
for metals,

E_i = the energy of the primary above which only ionization and
no displacements are produced, approximately 56 kev for iron.

Now let us compute the number of displacements produced under some typical reactor conditions. Assume a monoenergetic neutron flux of 10^{13} neutrons $\text{cm}^{-2} \text{sec}^{-1}$, all having an energy of 1 Mev, and a cross section of $3 \times 10^{-24} \text{cm}^2$. Allow the irradiation to continue for one year (approx 4×10^7 sec). Under these conditions

$$N_r/N_o = 10^{13} \times 4 \times 10^7 \times 3 \times 10^{-24} = 1.2 \times 10^{-3}.$$

About 0.1% of the atoms become primary knock-on atoms in a year.

The maximum energy transmitted to the primary is (for iron $M = 56$)

$$E_{\max} = 4.1/56 \approx 0.07 \text{ Mev} .$$

This is above the ionization energy, so the number of displacements per primary is

$$N_r = \frac{56,000}{2 \times 25} \approx 10^3 \text{ displacements} .$$

On this basis, each atom has been displaced once on the average during the year of irradiation. The accuracy of a calculation such as this is certainly questionable; however, it serves to indicate that a large number of atoms are displaced in a metal under typical reactor conditions. Thus far the theory does not consider the configuration in which the atoms find themselves after they have been displaced. For this purpose, dynamic computer calculations have been made that simulate the atoms in a crystal during the neutron bombardment (10,11). These results indicate that many complicated events may occur. Figure 3 shows some of the possibilities.

It is important to realize that the displaced atoms are not produced homogeneously throughout the material. For an individual collision the defects reside in a small volume around the track of the primary knock-on, which typically extends a few tens of perhaps hundreds of angstroms. This volume is termed a displacement cascade, but in reality it may be composed of subcascades produced by secondary knock-ons. Note too the distribution of vacancies and interstitial when the cascade is not uniform. In general, the interstitials are displaced outward, leaving a vacancy-rich core in the center of the cascade.



Fig. 3. A Two-Dimensional Illustration of the Possible Neutron-Nucleus Interactions In Crystalline Materials. In the upper left the neutron transfers a large amount of energy to the knock-on atom, which then produces two displacement cascades. The upper cascade has, in the shaded area, a defocusing sequence and in the lower cascade the shaded area indicates a focusing sequence. The neutron represented by b undergoes a glancing collision on transferring a small amount of energy to the knock-on atom, and no cascade is produced. The neutron represented by c is absorbed by the nucleus which then emits a gamma ray of sufficient energy to displace the atom. For a discussion of the structure of the damaged region, see D. K. Holmes, Current Problems in the Theory of Radiation Damage, paper presented at AIME Symposium on Radiation Effects, Asheville, N. C., September 1965, to be published in proceedings.

Thus, in the absence of thermal rearrangement of the displaced atoms we should expect to find large numbers of single point defects (vacancies and interstitial atoms), small clusters of a few point defects, and larger regions rich in vacancies.

The annealing of these complicated arrays of defects is not very well understood. Measurements of the change in resistivity of metals indicate that the major portion of those defects that contribute to resistivity disappear rapidly at temperatures of $0.35T_m$ and $0.5T_m$ for the body-centered cubic and face-centered cubic metals, respectively, where T_m is the melting point in degrees absolute (12). Annealing of some of the types of defects occurs below room temperature so that the final distribution of defects is a sensitive function of the temperature of irradiation and postirradiation testing. At temperatures above the fractions of the melting points quoted above, we would expect this type of radiation damage to anneal out.

The other event we shall discuss is the transmutation reaction between a neutron and the nucleus of an atom. Table 2 lists the reactions and their cross sections for a number of important cases. We see that helium and hydrogen may be produced in metals through neutron reactions both with impurities in the metals and with the major alloying elements. Alter and Weber (13) have made calculations of the amounts of hydrogen and helium produced in various materials and concluded that for the iron- or nickel-base alloys used as fuel cladding, approximately 100 ppm He and a few thousand parts per million hydrogen would be produced in a fast reactor in a few years' operation. In addition to these transmutation reactions producing gaseous products, other possibilities

Table 2. Transmutation Reactions in Metals

Nucleus	Reaction	Cross Section (barns) ^a	Neutron Energy Associated with Cross Section
¹⁴ N	(n,α)	41	Fission
¹⁰ B	(n,α)	3800	Thermal
	(n,α)	635	Fission
⁵⁶ Fe	(n,α)	0.35	Fission
	(n,p)	0.87	Fission
⁵⁸ Ni	(n,α)	0.5	Fission
	(n,p)	111	Fission

^a1 barn = 10⁻²⁴ cm².

exist in which solid impurities are produced. In most cases cross sections are low enough that appreciable quantities are not formed. An important exception is the ¹⁹⁷W (n,β) ¹⁹⁷Re reaction. As higher power density reactors are developed, this may become an important problem area.

OBSERVATIONS OF IRRADIATED MATERIALS

Since the initial work of Silcox and Hirsch (14), transmission electron microscopy has been used extensively to characterize structural changes resulting from irradiation. The results appear to depend critically not only on the irradiation conditions and on the material examined, but also strongly on its purity. Consequently there still is controversy

over the identity of defect clusters formed by low-temperature irradiations. Most of the investigations have been confined to high-purity single-phase materials, with little attention paid to complex engineering materials or to high-temperature irradiations. We will attempt here to summarize the essential features of the findings and to show the extent and very broad nature of the problem.

Black spots of the order of a few tens of angstroms in diameter, often called the "Black Death," appear in transmission electron micrographs of metals irradiated at low temperatures ($< 0.35T_m$), as is illustrated in Fig. 4. Recent quantitative studies by electron microscopy of irradiated face-centered cubic metals have at various times shown them to be exclusively vacancy clusters and loops (15,16), interstitial clusters and loops (17,18), or mixtures composed of small vacancy clusters and larger resolvable interstitial loops (19,20). Differences still have

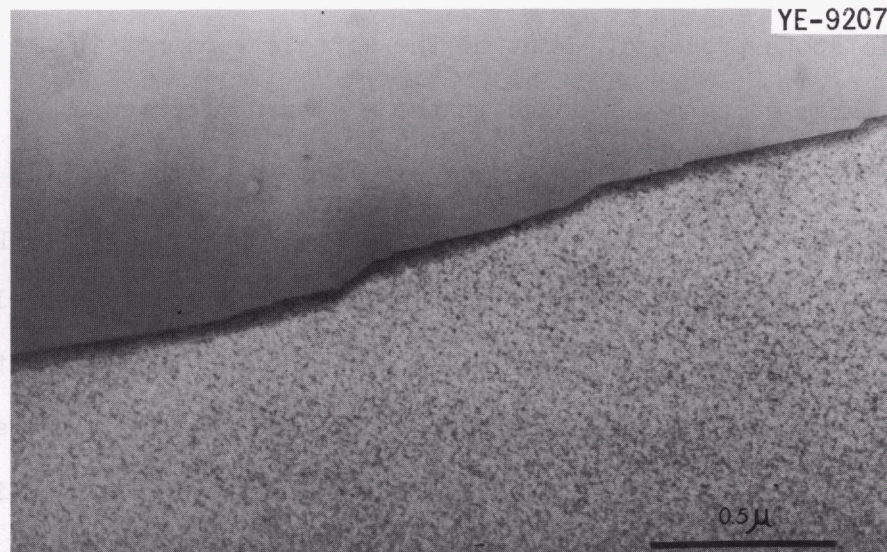


Fig. 4. Transmission Electron Micrograph of Type 304 Stainless Steel Irradiated at 93°C. The black spots are defect clusters produced by the irradiation.

not been settled, and we must at this point conclude that all can probably be formed but that individual circumstances determine which occur for a particular situation.

Merkle (21,22) irradiated thin foils of copper and gold with heavy ions in order to study damage from individual knock-on events. In gold he concluded that each knock-on having energy greater than 27 kev produced a detectable spot (> 20 A in diameter) and that the size of the spot increased with increasing knock-on energy up to a maximum diameter of about 150 A. In copper, however, not every knock-on above a critical energy resulted in visible damage. Merkle explained this in terms of the distribution of defects in the displacement cascades. The range of a 50-kev atom in copper is about four times that of one in gold (250 vs 60 A), so that the defects in gold are confined to a relatively small volume, while in copper they are spread out in relatively widely spaced subcascades. Only when two or more of these overlapped were detectable spots produced. Most of the defects were not in the form of clusters large enough to resolve in the electron microscope.

Howe et al. (23) performed some experiments in which foils of aluminum, copper, and silver were irradiated by heavy ions at approximately 20°K in the electron microscope. Spots identified as vacancy clusters or Frank loops parallel to $\{111\}$ or $\{110\}$ were formed, indicating that vacancy-rich zones collapse to dislocation loops at this temperature. The interstitials escaped from the foils, were trapped at imperfections, or frozen in the lattice individually or in groups too small to be observed. In bulk copper irradiated at higher temperatures, Makin et al. (19,20) identified large, well defined interstitial loops in addition to the

vacancy-induced spots. Since such large loops are not always observed (15,16), it is possible that their nucleation and growth are controlled by impurities. Makin et al. were able to correlate the radiation-induced hardening with the small vacancy clusters or loops.

Koppenaar et al. (24,25) showed that the addition of certain substitutional solute atoms to copper eliminated the interstitial loops but did not influence the hardening mechanism, in agreement with the previous conclusion that the vacancy clusters or loops were responsible for the strengthening.

In the body-centered cubic crystal system the situation is quite different. The fluence at which observable clusters appear and their distributions both are sensitive functions of interstitial impurity content. For molybdenum (26) irradiated at less than 100°C, the clusters were more widely distributed in the purer specimens; upon annealing at elevated temperatures (approx 900°C) large, interstitial loops were observed. Similar results were obtained on iron (27). Eyre and Downey (28) found two components of damage in molybdenum specimens irradiated at 200°C, dots and irregular dislocation lines believed to be segments of large clusters. Upon annealing, the dot-like structure evolved into identifiable vacancy loops. These results indicate that the clusters are nucleated heterogeneously on impurity atoms and that the identity of the clusters depends on the mobility of defects at the irradiation temperature.

Electron microscopy observations must necessarily be made at relatively low doses where defect images do not overlap or interfere with one another. There is evidence (29) that hardening mechanisms and annealing

behavior are altered at high fluences suggesting that the defect clusters grow more complex with age or increasing fluence. In addition, most fundamental investigations have been made on relatively high-purity, single-phase materials irradiated at low temperatures where competing and complicating precipitation reactions do not occur. Engineering materials in which ductility considerations are important have received relatively little attention from the microscopists. Therefore the following discussion should be considered as an introduction to the more complex problem of damage in structural materials irradiated to high fluences at temperatures up to 800°C.

Wilsdorf and Kuhlmann-Wilsdorf (30) in a study of type 304 stainless steel irradiated at reactor ambient temperature to fluences of up to 10^{19} neutrons/cm² were unable to detect any visible defect clusters although the material was hardened and dislocation motion modified. They suggested that invisible vacancy-rich regions were responsible for the changes. Armijo et al. (31) were able to detect a dot-like damage structure in the same material irradiated at 43 and 343°C to fluences of 10^{20} and 10^{21} neutrons/cm², respectively. The defects were considerably larger in the specimen irradiated at the higher temperature to the higher dose. Bloom et al. (32) correlated the defect structures in type 304 stainless steel irradiated to a fluence of 7×10^{20} neutrons/cm² with strength properties. At irradiation temperatures of 300°C and less the damage consisted of black spots which Bloom et al. concluded were probably vacancy in character (Fig. 4). The spots appeared to grow slightly in size and decrease in density with increasing irradiation temperature, although the defect density was too high to allow quantitative estimates of either

to be made. After irradiation at 371°C, the yield stress and the density of spots both decreased markedly (Fig. 5). Irregularly shaped planar defects, probably precipitates, developed, but these were widely enough spaced that they did not very greatly modify the yield stress. More extensive precipitation, including a heavy layer along grain boundaries, was observed at an irradiation temperature of 454°C (Fig. 6). The dot-like defect clusters were completely absent. Arkell and Pfeil (38) also showed that massive carbide developed in a niobium-stabilized steel (20% Cr-25% Ni) irradiated to comparable doses at temperatures of 350 and 750°C.

At irradiation temperatures of 650°C and above, the inert-gas atoms formed by nuclear transmutations have been observed to precipitate as bubbles. Rowcliffe *et al.* (34) observed heterogeneous precipitation in clusters on grain boundaries of specimens irradiated at 650°C. Homogeneous

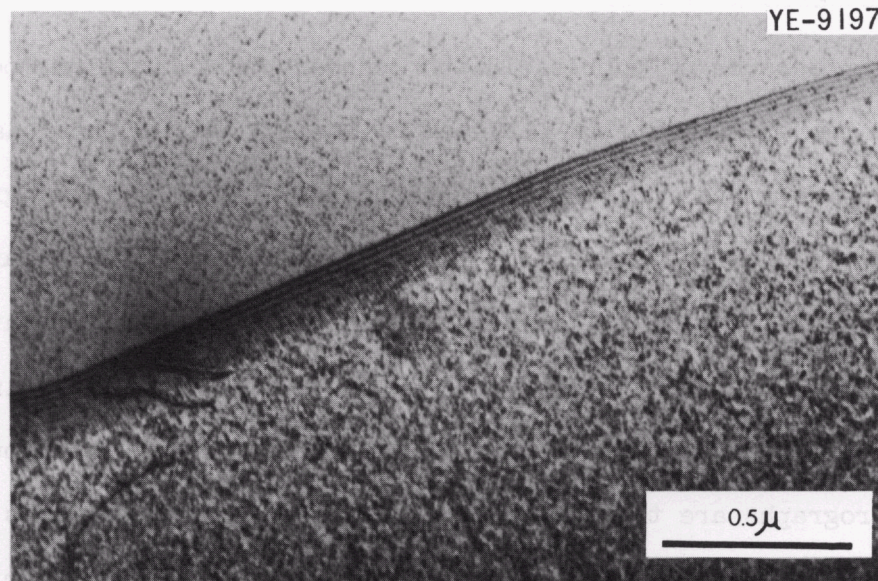


Fig. 5. Transmission Electron Micrograph of Type 304 Stainless Steel Irradiated at 177°C. The spots are larger and more widely distributed than those in the specimen irradiated at 93°C (Fig. 4).

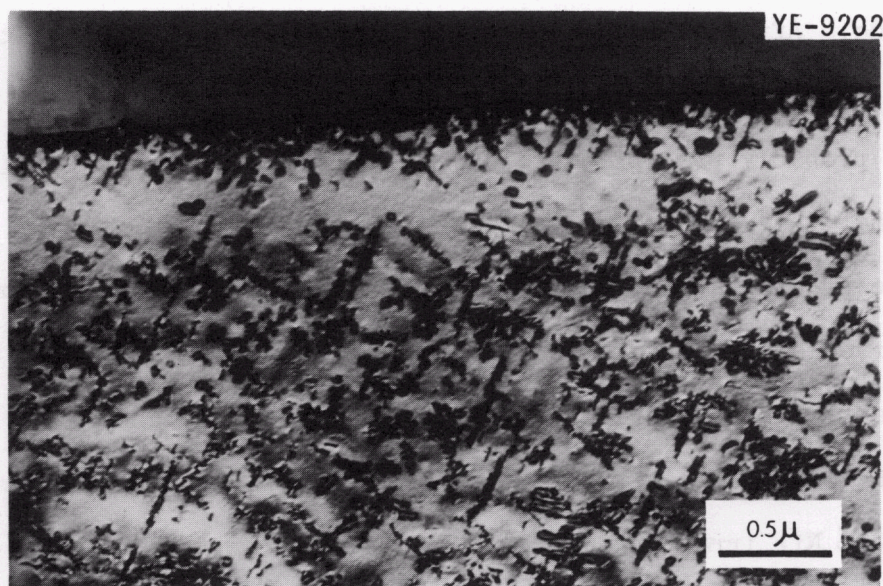


Fig. 6. Transmission Electron Micrograph Showing Precipitate Particles Formed in Type 304 Stainless Steel during Irradiation at 454°C. Note the denuded zone adjacent to the boundary and the extensive precipitation on the boundary.

precipitation within the grains occurred in these specimens annealed at 800°C or irradiated at 750°C. Growth of bubbles under stress was detected in tensile tests at 750°C.

The appearance of bubbles in the boundary of a titanium-modified type 304L stainless steel is illustrated in Fig. 7. In this case the bubbles in the boundary are larger than those in the adjacent grains, and they have well defined polyhedral shapes. The black circular area in the figure is a precipitate particle having several small bubbles attached to it. In Fig. 8 bubbles on the boundary are smaller than those in the adjacent grains, and a zone denuded of bubbles surrounds the boundary. These micrographs are typical of areas in which helium contents were high enough for homogeneous nucleation of bubbles to occur. In areas of

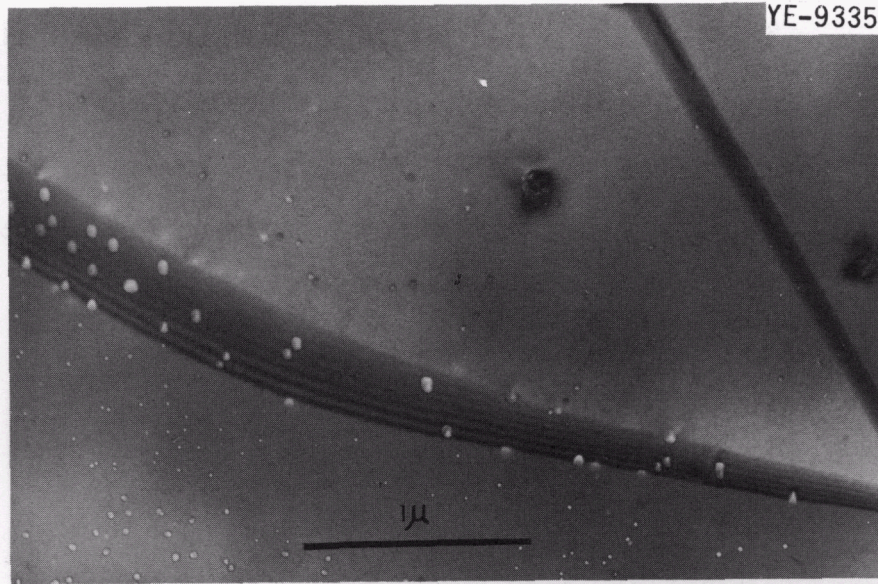


Fig. 7. Transmission Electron Micrograph of Titanium-Modified Type 304 Stainless Steel Irradiated at 800°C. The light areas are helium gas bubbles resulting from the reaction of thermal neutrons with ^{10}B . The bubbles clearly have polyhedral shapes. The small black circle near the center of the micrograph is a precipitate particle having several small bubbles attached to it.

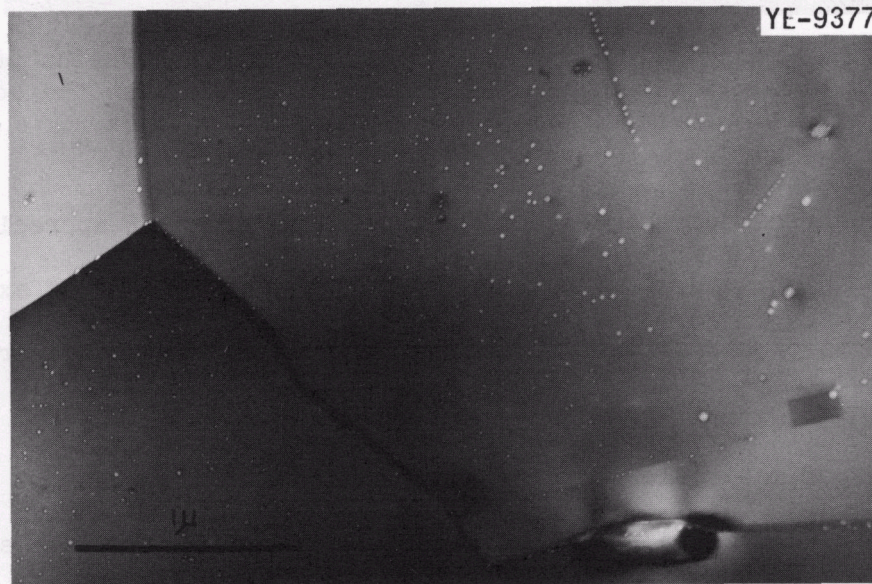


Fig. 8. Another Area of the Specimen Shown in Fig. 7. Notice the zone denuded of bubbles adjacent to the diagonal grain boundary. The chains of bubbles in the upper right-hand corner of the figure lie along dislocation lines.

low gas content bubbles are located at structural irregularities such as along the triple grain junctions approaching a quadruple point, as is shown in Fig. 9. In addition, dislocations, dislocation nodes, and dislocation-grain-boundary intersections are preferred bubble nucleation sites.

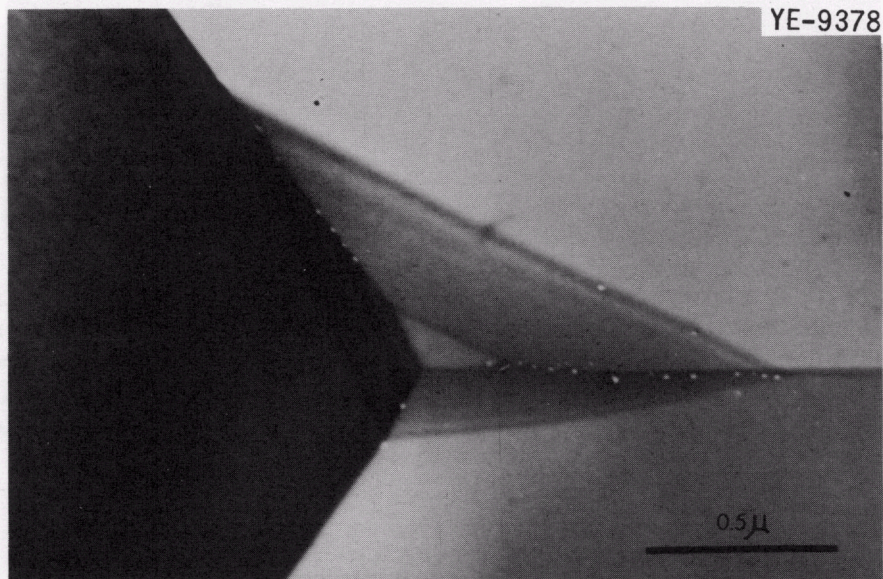


Fig. 9. Transmission Electron Micrograph Showing Chains of Bubbles Lying Along Triple Grain-Boundary Junctions. Notice that the boundary surfaces near the junctions are generally free of bubbles.

Although solid transmutation products are formed in appreciable quantities in structural materials after high thermal neutron exposures, their effects on microstructure and mechanical properties have received little attention. Wittels et al. (35) characterized structural changes in a number of materials in which greater than 10% of the atoms present were transmuted. Since the irradiations were carried out at less than 100°C, nonequilibrium crystal structures were frozen in. No mechanical or physical properties were determined. Motteff et al. (36) determined creep properties at 1100°C of tungsten irradiated to produce 2.5% Re

atoms and 0.25% Os atoms as transmutation products. They found that the minimum creep rate decreased with increasing exposure, but the creep rate was related to the thermal fluence (rhenium plus osmium concentration) rather than to the fast neutron damage. Transmission electron microscopy showed the presence of a few large loops, up to 2000 Å in diameter, but no structural change associated with the transmutation products. Evidently solid solution effects rather than structural changes modified the creep properties, although impurity atom-point defect complexes could have been responsible.

Neutron fluence and neutron flux are additional variables that may influence the nature of the damage structure. The results just described apply to irradiations in thermal reactors where the fast flux is a few times 10^{14} neutrons $\text{cm}^{-2} \text{sec}^{-1}$, or less. In fast reactors where the flux is an order of magnitude higher and comparably higher doses can be achieved, additional complications result. At irradiation temperatures of 300°C and less, Cawthorne and Fulton (37) reported black-spot damage, although the density of defects was too high to allow analysis of their nature. At irradiation temperatures between 350 and 560°C, spherical cavities ranging up to 500 Å in diameter were observed, which occupied up to 2% of the volume of the specimen. The volume of voids was several orders of magnitude too great to be accounted for by helium bubbles. Cawthorne and Fulton suggested that the voids developed either from stress-assisted growth of bubbles or vacancy condensation due to the high vacancy supersaturation in the high fast flux irradiation.

In addition to the defects resolved by electron microscopy, Ralph et al. (38) using field ion microscopy detected smaller clusters containing up to about 200 vacancies. In irridium, spherical clusters and collapsed loops were observed as well as depleted zones in which 30 to 40% of the lattice sites were unoccupied. In tungsten only vacancies, divancancies, and clusters containing less than about 100 vacancies were imaged. In neither case were interstitial loops detected, although under the irradiation conditions employed their density would have been low enough to present a sampling problem with this technique. The important point is that in addition to containing the large clusters and loops, the lattice of an irradiated metal is riddled with vacancies, divacancies, small clusters and vacancy-rich zones.

PLASTIC FLOW AND FRACTURE IN IRRADIATED MATERIALS

Dislocation-Defect Interactions

Which of this complex spectrum of defect configurations governs mechanical properties changes is an unanswered question. Measurements by Diehl and Ast (39) of the critical shear stress change on annealing pure nickel that had been irradiated at 4.2°K showed a monotonic decrease in the hardening with increasing annealing temperature. This indicated that the defect configuration primarily responsible for the hardening results directly from the knock-on event and not from subsequent thermally activated clustering or rearrangement of the defects produced. On the other hand, the yield stress change in stainless steel (32) reached a maximum at an irradiation temperature of 200°C, suggesting that more complex defect configurations, when they form, are more potent strengtheners.

The presence of the defect structure introduced by irradiation alters not only the strength but also the external appearance of deformed metals. First, deformation is usually initiated near one of the grips in a tensile test and then spreads over the specimen as a Luders band; and second, the slip steps within the deformed region are deep and relatively widely separated by undeformed areas, as contrasted with a uniform distribution of fine slip bands in unirradiated materials. Transmission electron microscopy (40,41,42,43) of such crystals has shown channels in which the radiation-induced defect structure has been eliminated (see Fig. 10). These defect-free channels correspond to the deep slip steps. The interpretation is that glide dislocations sweep out or in some manner destroy the radiation-induced defect structure. The channels are generally clean except for deformation-induced tangles and dipoles. The radiation defects are completely eliminated from the channels (43) and not simply pushed to the edge of the channel, as was originally suggested (40). Sharp (43) examined annealed specimens containing channels and found no development of structure within the channels, as would be expected if they contained a high density of point defects or point defect clusters below the resolution limit of the microscope. The mechanism by which the moving dislocations destroy the radiation-produced defects has not been determined. The shears associated with the channels determined by measuring the slip line offsets correspond to the passage of two or three dislocations on each plane within the channel, so ample opportunity exists for dislocations to remove all the defects present.

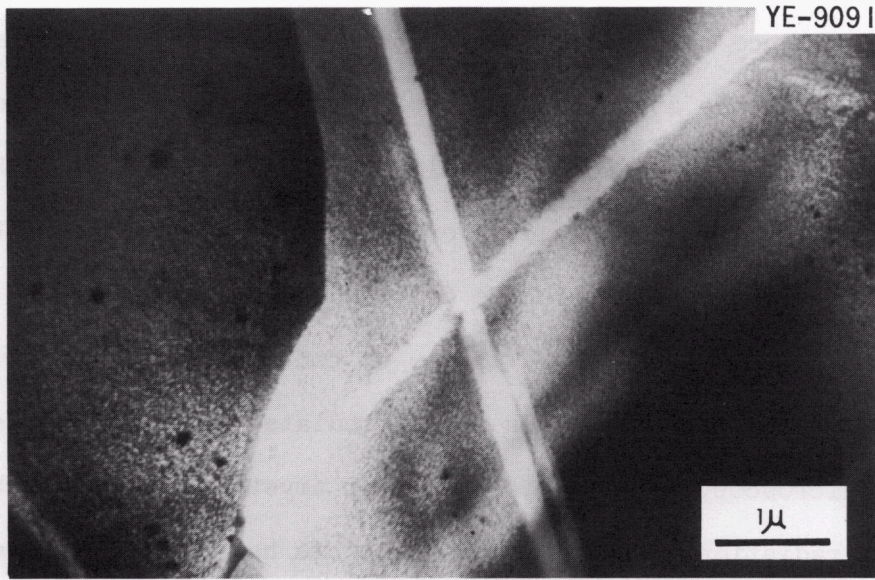


Fig. 10. Transmission Electron Micrograph of Irradiated Molybdenum Deformed Lightly at Room Temperature. The white bands are channels in which the defect clusters have been swept out by moving dislocations.

The channels gradually fill with tangles and deformation-induced debris, which ultimately halt the deformation in the channels. Sharp (43) observed a higher density of debris existing on a smaller scale in the channels than in unirradiated material, but attributed this to the higher stress at which the slip band developed. During the latter stages of deformation the slip line pattern of irradiated crystals appears similar to that of unirradiated materials.

Seeger (44) suggested that the defect clusters harden the lattice by providing obstacles which moving dislocations must cut with the combined aid of the applied stress and thermal fluctuations. The defects as a result of this chopping are gradually reduced in strength and ultimately destroyed or eliminated by the dislocations leading to the channels that are observed.

Makin and Sharp (45) pointed out that in irradiated materials relatively few slip lines are observed, indicating that few sources are activated, that full-grown slip lines form dynamically in times of the order of a millisecond, and that partially formed slip lines are not observed. They proposed on the basis of elimination of the defects by moving dislocations that the critical stress to form a slip band is the stress to operate a source in the environment of the defect structure. Subsequent loops can be formed more easily, since the first one, so to speak, clears a path for them. A pileup then forms and expands, creating the cleared channel very rapidly at the high stress levels necessary to generate the first dislocation. The result is creation of a soft zone in a hardened material in which extensive localized shear occurs in a short time until work hardening halts the deformation.

Ductility and Mechanical Properties Effects at Low Temperatures

A general behavior pattern is emerging concerning the response of the mechanical properties of a wide variety of metals and alloys to neutron irradiation. We shall discuss the general behavior, give some specific examples, and relate the changes in ductility to observations using electron microscopy.

A systematic study (46) of the effects of irradiation and testing temperatures on the postirradiation mechanical properties of stainless steels indicates qualitatively the behavior shown in Table 1. We observe differences in the characteristics of these alloys depending on both the irradiation temperature and the testing temperature. Further

work has indicated that the ductility (elongation) as a function of irradiation and testing temperature decreases to a minimum, rises, and then decreases again (see Fig. 11).

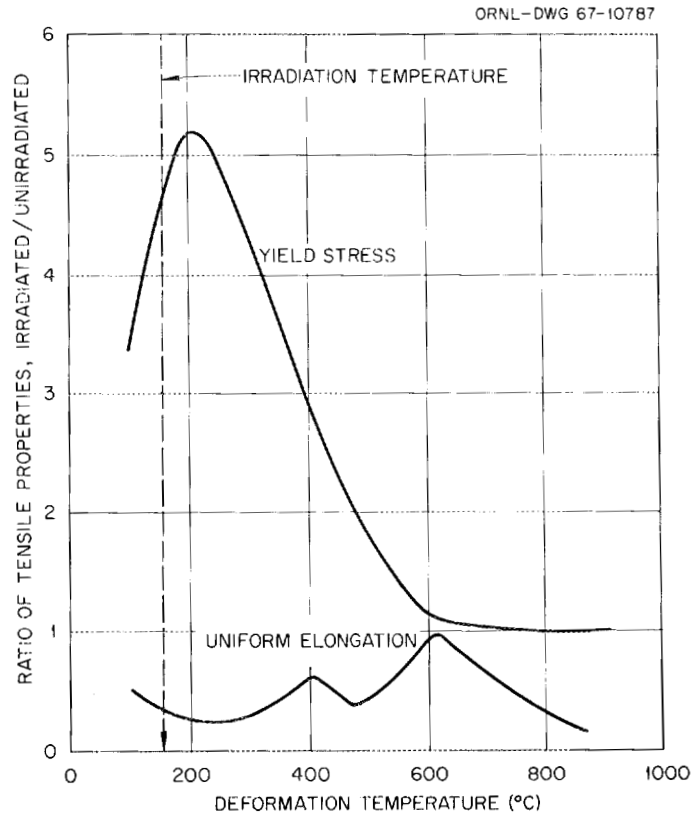


Fig. 11. The General Behavior of Stainless Steels after Irradiation at Low Temperatures.

There is other evidence (46,47,48) that the minimum in the temperature range of 200°C occurs only after the material has been exposed to relatively large neutron fluences. Figure 12 shows how stainless steel behaves as a function of neutron exposure at various temperatures and illustrates that the minimum in ductility at 200°C develops only after a neutron exposure of approximately 5×10^{20} neutrons/cm².

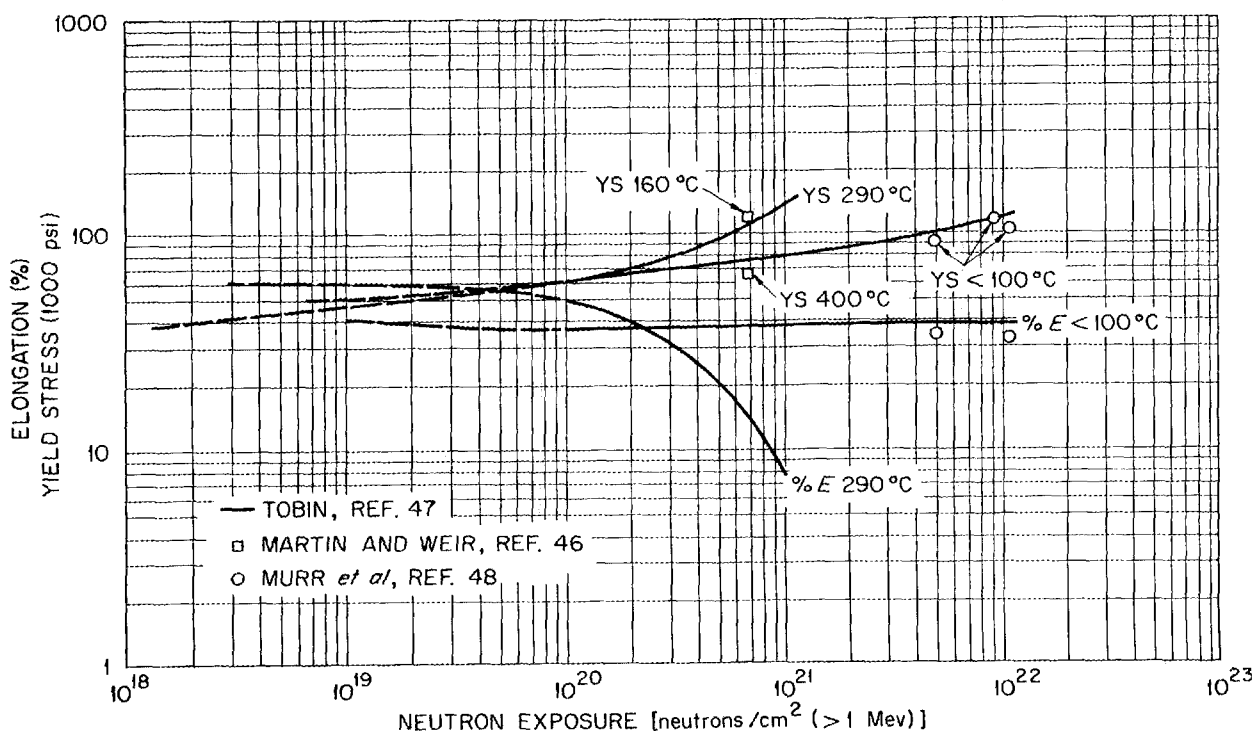


Fig. 12. Room-Temperature Properties of Annealed Stainless Steel after Irradiation at Various Temperatures.

Now let us first examine this low-temperature behavior more closely. Stress-strain curves obtained (32) at room temperature after irradiation at various temperatures in this low-temperature range are shown in Fig. 13. Observe that for temperatures of 300°C and lower the yield stress rises with irradiation temperature and the elongation decreases. The true fracture stresses and strains are not affected, however. After irradiation at 454°C the elongation has increased again but the fracture stress and strain are lower than in the other tests indicating an effect having different characteristics than in the other tests. The work hardening exponents in the plastic range (see Fig. 14) are consistent in all cases with the uniform and total elongation values, although the specimen irradiated at 454°C is anomalous.

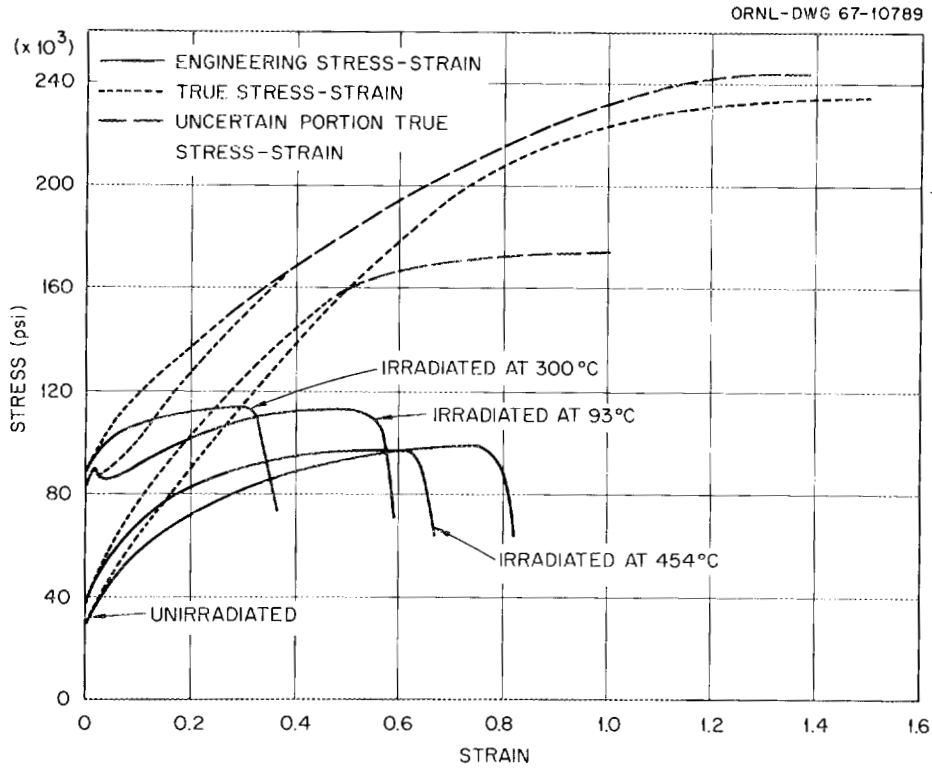


Fig. 13. The Engineering and True Stress-Strain Curves for Type 304 Stainless Steel at Room Temperature, Tested in the Unirradiated Condition and after Irradiation at Various Temperatures.

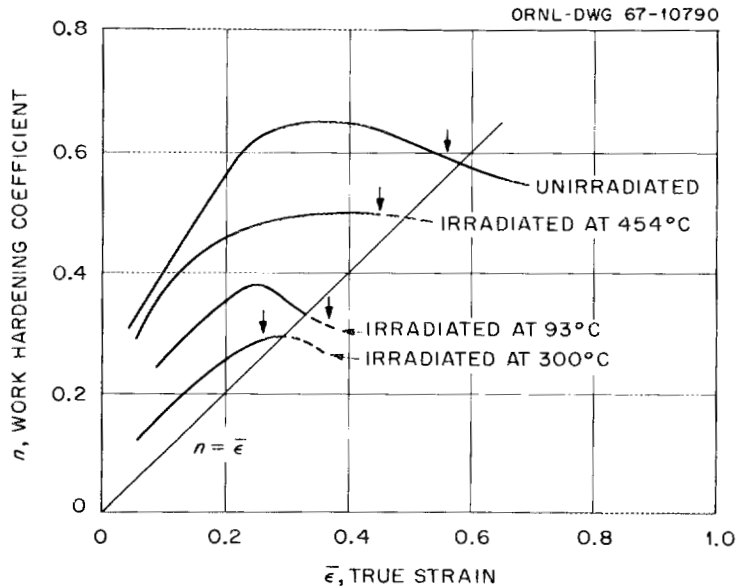


Fig. 14. The Work-Hardening Characteristics Associated with the Stress-Strain Curves Shown in Fig. 13.

This behavior can be explained in terms of the microstructural changes discussed earlier and of the interaction between dislocations and the radiation induced defect clusters. Microstructural observations on stainless steel (30,31,32) show that a more complex defect configuration develops at fluences above 10^{20} neutrons/cm² and that its size and spacing are critical functions of the irradiation temperature. These, in turn, determine the strength and work hardening characteristics of the material. The observations that dislocations remove the defect clusters (40,41,42,43) and that in irradiated materials slip is confined to narrow channels provide an explanation for the reduced work-hardening coefficients of the irradiated materials. The channeling produces a soft zone in a very hard material in which very extensive slip occurs and by limiting the number of sources or slip systems makes more difficult interactions between dislocations and tangling which normally lead to work hardening. Figure 15 illustrates the narrow regions to which slip is confined in stainless steel irradiated at 121°C and deformed 10% by rolling at room temperature. The defect structure is still clearly visible in the region between the slip bands.

The anomalous behavior of the specimen irradiated at 454°C is not related to displacement damage but is probably due to the precipitate particles formed during irradiation. Unlike the defect clusters they are not removed by the dislocations but rather provide permanent obstacles and sites for tangling. In addition numerous sources and slip systems are active, leading to the tangled configuration pictured in Fig. 16. The reduced fracture stress and strain possibly arise from the extensive grain-boundary precipitation that also occurred.

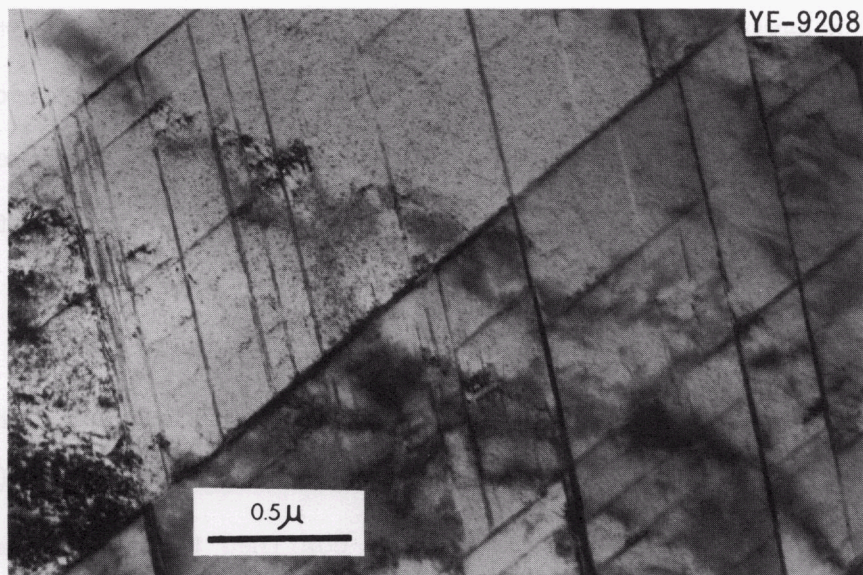


Fig. 15. Transmission Electron Micrograph of Type 304 Stainless Steel Irradiated at 121°C and Deformed 10% by Rolling at Room Temperature. All the deformation has been confined to the dark bands; the radiation-induced defect clusters can still be seen between the bands.

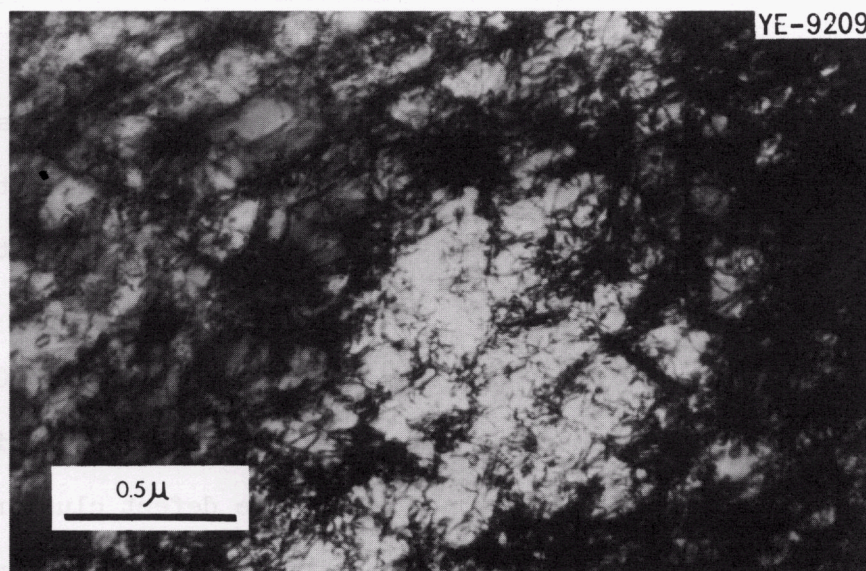


Fig. 16. Transmission Electron Micrograph of Type 304 Stainless Steel Irradiated at 454°C and Deformed 10% by Rolling at Room Temperature. Compare the uniform distribution of tangled dislocations with the localized slip bands produced in specimens irradiated at a lower temperature (Fig. 15).

Although this discussion is limited to the behavior of stainless steel, it illustrates the nature of the problem and the complexities introduced by microstructural changes introduced by irradiation.

Ductility at High Temperatures

At high temperatures of deformation where the materials tend to fracture intergranularly (in the absence of irradiation), a large number of iron- and nickel-base alloys are observed to be severely embrittled by neutron irradiation (49,50). As is indicated in Table 1, the embrittlement takes the form of reduced elongation and reduction of area values. The magnitude of the high-temperature embrittlement is sensitive to the alloy composition and structure, the test temperature, the strain rate, and the irradiation conditions. Examples of the effects of some of these variables are illustrated in Figs. 17 and 18. Figure 17 illustrates the dependence in the form of a plot of fracture elongation in stress-rupture and tensile tests as a function of the rupture life and Fig. 18 shows the effect of grain diameter on elongation.

At these temperatures lattice damage would quickly anneal out, so that we must look elsewhere for the source of the problem. Indirect evidence that bears on the causes for the high-temperature embrittlement has been obtained. For example, Harries and Roberts (51) showed that the embrittlement was predominantly a function of thermal-neutron exposure at low doses of fast neutrons. Martin *et al.* (52) related the embrittlement to the helium generated by the thermal-neutron $^{10}\text{B}(n,\alpha)$ reaction and showed that at very low concentrations of boron in type 304 stainless steel, the contribution of helium from (n,α) reactions between high-

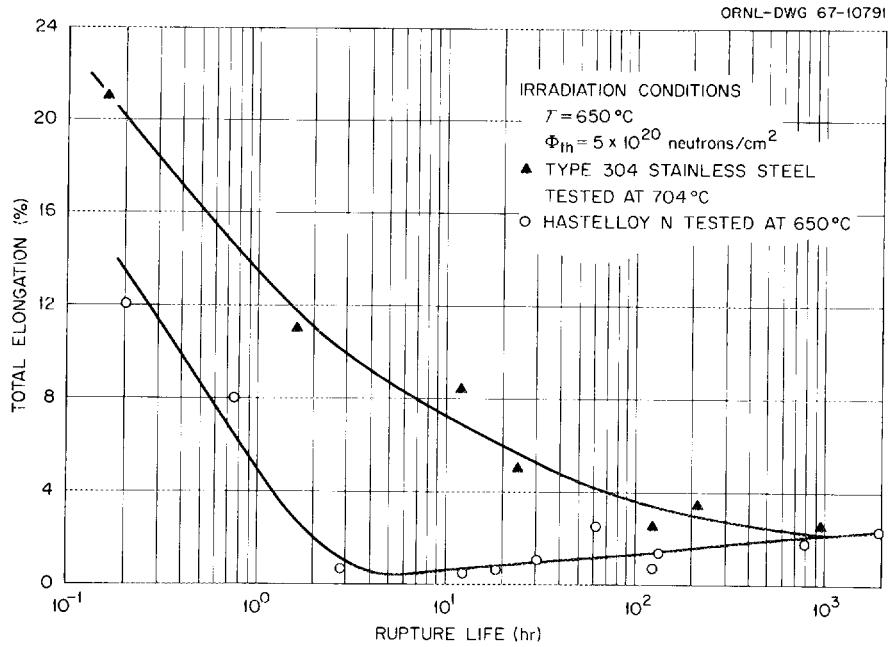


Fig. 17. The Postirradiation Ductility of Hastelloy N and Type 304 Stainless Steel as a Function of the Rupture Life in Stress-Rupture and Tensile Tests.

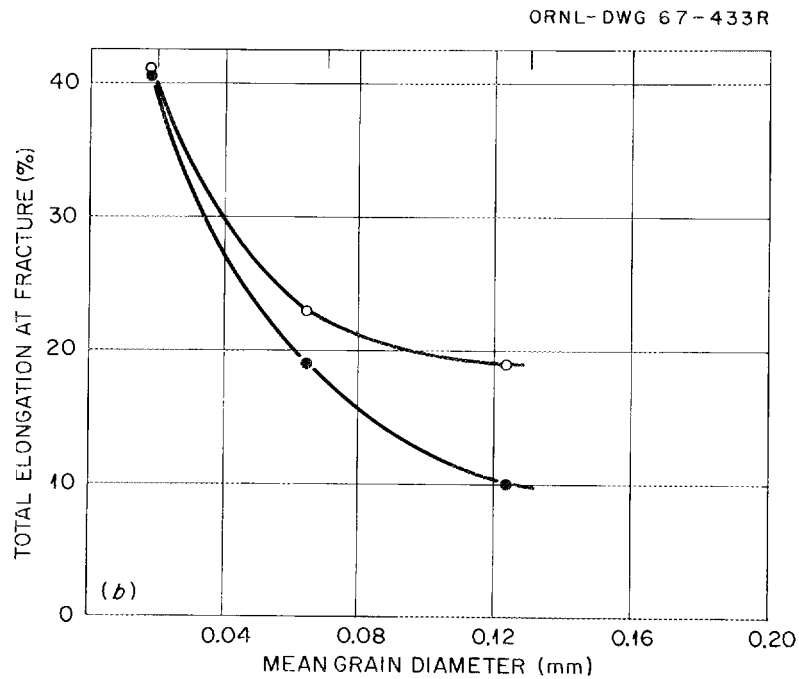


Fig. 18. The Effect of Grain Size on the Total Elongation of Type 304 Stainless Steel at 700°C after Irradiation.

energy neutrons (fast neutrons) and iron, nickel, and other constituents in the alloy was also important (see Table 2). Figure 19 shows that the ductility, after irradiation of type 304 stainless steel containing various amounts of boron and subjected to various doses or irradiation, is a function of the total helium content from both the thermal $^{10}\text{B}(n,\alpha)$ reaction and the high-energy (n,α) reactions. Higgins and Roberts (53) reported that the ductility of an alloy at high temperatures was reduced through the injection of helium by means of cyclotron bombardment with alpha particles.

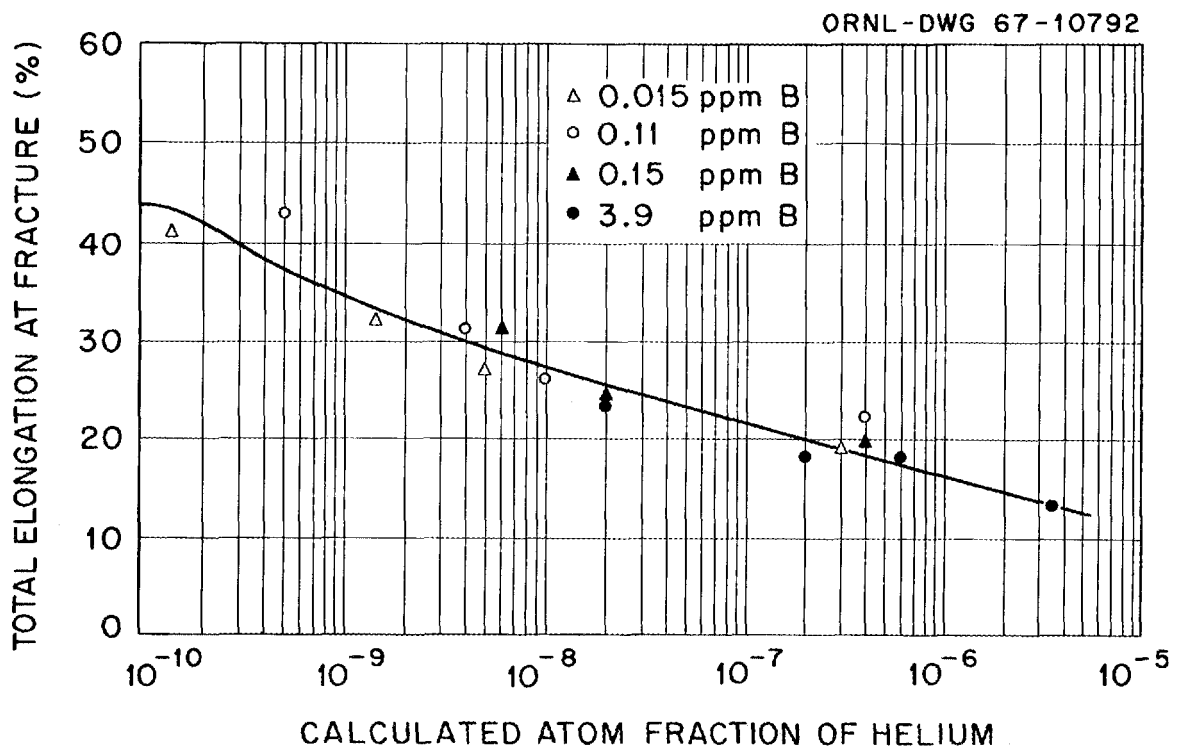


Fig. 19. The Elongation at Fracture of Type 304 Stainless Steel Containing Various Amounts of Boron and Exposed to Four Radiation Doses, Ranging from 1×10^{18} to 5×10^{20} neutrons/cm². The elongation is shown to be a function of total concentration of helium produced by both high-energy and thermal neutrons. The specimens were tested at 700°C after irradiation at 50°C in the Oak Ridge Research Reactor. Boron concentrations (in parts per million): open triangle, 0.015; open circle, 0.11; solid triangle, 0.15; solid circle, 3.9.

That helium, or any other atomic species, at a concentration of 10^{-9} (see Fig. 19), could produce a pronounced effect on the ductility of a metal is difficult to imagine. However, the noble gases are very insoluble in metals. Rimmer and Cottrell (54) have estimated the energies required for solution of the inert gases in copper. The least energy is required when the gas atom is in a vacant lattice site of the metal; for helium, the value is about 1 ev. Cottrell (55) indicates that the equilibrium concentration C of gas in solution is

$$C = (P/NkT) \exp(-F/kT) , \quad (21)$$

where

P = pressure,

N = the number of solvent atoms per unit volume,

T = temperature,

k = Boltzmann's constant,

F = the energy of solution.

At a temperature of 700°C the concentration of helium is less than 10^{-9} at a pressure of 1 atm. If there are not enough vacant lattice sites for the helium atoms, then the energy of solution is approximately 2.5 ev and the solubility is less than 10^{-15} at a pressure of 1 atm.

Behavior of Gases, Bubbles, and Grain Boundaries

In understanding the influence of helium on the fracture process, two points must be considered: (1) the distribution of the helium and (2) the response of the helium (bubbles) to a tensile stress. Earlier we showed that at irradiation or test temperatures above about half the absolute melting

temperature helium bubbles form in stainless steel. In thermal reactors, where the helium is generated by the $^{10}\text{B}(n,\alpha)$ reaction, the distribution of helium largely reflects the distribution of the boron, since the helium recoil range is only about $2\ \mu$. Since boron has been frequently observed to inhabit the grain-boundary regions, such areas may have concentrations well above mean levels. The mechanism of diffusion of helium is not established, but some feeling exists that small bubbles ($< 25\ \text{A}$ in diameter) may be the most rapidly diffusing species. Such bubbles presumably would migrate randomly until they reach traps or collide with other bubbles, coalescing to form bubbles too large to diffuse further. At low helium concentrations we would suspect that collisions would be rare and that bubbles would ultimately reach grain boundaries where they would be trapped. They still would be free to move in the surface of the boundary until they collide with other bubbles or reach the more stable triple grain-boundary junctions (Fig. 9). At low gas concentrations the largest bubbles probably exist at triple junctions, but smaller bubbles are likely distributed over the grain boundary. At higher concentrations larger bubbles form in the boundary, and precipitation within the grains may occur. In a 25% Cr-25% Ni-Ti stainless steel containing approximately 4 at. ppm He, Rowcliffe et al. (34) observed on boundaries bubbles ranging from 30 to 80 A in diameter after irradiation at 650°C . After irradiation at 750°C coarsening occurred such that observed bubbles ranged between 60 and 180 A in diameter. The specimen pictured in Fig. 7 contained about 15 ppm He and after irradiation at 800°C contained grain-boundary bubbles ranging up to 650 A in diameter.

Barnes (56) proposed that stress-induced growth and linking of these bubbles to form cracks was the cause of the high-temperature ductility loss. Consider a bubble on a grain boundary in the absence of an external stress. Removal of an atom from the surface of the bubble increases the surface energy $2\gamma/r_0 \Omega$ and does work $P_0 \Omega$ in expanding the gas, where Ω is the atomic volume, r_0 the radius of the bubble, and P_0 the gas pressure in the bubble. Equilibrium exists when these terms are equal

$$P_0 = 2\gamma/r_0 . \quad (22)$$

If a stress T_m is applied, additional work $\sigma_n \Omega$ is done in transferring an atom from the bubble to the grain boundary outside the bubble. The equilibrium condition becomes

$$\sigma + P = \frac{2\gamma}{r} , \quad (23)$$

where $P < P_0$ and $r > r_0$. Since the product of pressure and volume remains constant, $P_0 r_0^3 = Pr^3$. Hyam and Sumner (57) showed that the stress in equilibrium with a bubble of radius r is given by

$$\sigma = \frac{2\gamma}{r} \left[1 - \left(\frac{r_0}{r} \right)^2 \right] . \quad (24)$$

This function has a maximum at $\sigma_c = 0.76 \gamma/r_0$. For stresses greater than σ_c equilibrium cannot be obtained, and unlimited bubble growth occurs. For a given stress, bubbles having a radius greater than $0.76 \gamma/\sigma$ will become unstable and expand indefinitely. Surface energies are not generally known with high precision, but values on the order of 1000 ergs/cm² are commonly quoted. Based on this value of γ , the

bubble radius above which unlimited growth occurs for a given stress is tabulated in Table 3. Bear in mind that the precise value of surface energy can change these values perhaps severalfold. The table indicates that the distribution of bubble sizes is important, for only those bubbles on the large end of the distribution will become unstable. It also shows that stress concentrations or stress transients can lead to expansion of bubbles much smaller than expected by the general level of the applied stress. The stronger engineering alloys are most likely to be embrittled by this mechanism, since they are used in relatively high-stress applications due to their ability to resist deformation processes.

Metallographic examination of irradiated materials strained at high temperatures shows that the appearance of the fracture is similar to that in unirradiated materials. At high stress levels wedge cracks are

Table 3. Initial Radius for Unlimited
Bubble Growth for Various Stresses^a

Tensile Stress (psi)	Radius (A)
1,000	1110
5,000	220
10,000	110
20,000	55
50,000	22
100,000	11

^aAssuming $\gamma \approx 1000$ ergs/cm².

formed, and at low levels cavitation is observed. The effect of irradiation is to reduce the strain at which rupture occurs. In the absence of irradiation, cracks and cavities are nucleated by plastic strain, but in irradiated materials, helium bubbles provide suitable nuclei without any prerequisite strain. Such bubbles can begin to grow into cracks at the onset of the test. The effect is greater at higher stress levels, since a larger fraction of the bubbles is capable of being expanded. However, since such bubbles probably grow by collecting vacancies at very high strain rates (stresses), they cannot expand rapidly enough to influence significantly the ductility or rupture life. Conversely, at very low stresses few bubbles will be large enough to be expanded. This accounts for the general behavior shown in Fig. 17.

The model of high-temperature radiation-enhanced embrittlement by helium gas bubbles, as proposed by Barnes (56), is formulated in terms of rupture by cavitation. This is observed at low stress levels, but enhanced wedge-type cracking is also observed at higher stress levels. Inhomogeneous bubble distributions, particularly chains of bubbles along triple grain junctions (Fig. 9), suggest that wedge cracks should be easily nucleated in irradiated materials. Such cracks could grow in the same manner in which they grow in unirradiated materials, the effect of the bubbles being simply to nucleate them with little prior strain, or their rate of propagation could be enhanced by the expansion of subcritical size bubbles by the stress concentration preceding the crack. It appears likely that gas bubbles enhance both the nucleation and the growth of cracks.

This picture of elevated-temperature radiation-induced embrittlement is consistent with the experimental observations summarized in Table 1. At these temperatures displacement damage anneals out, so that

irradiation has little effect on strength properties. However, helium generated by neutron reactions precipitates as bubbles, which enhance nucleation and perhaps propagation of cracks. The presence of bubbles does not alter the mode of rupture; bubbles merely nucleate cracks or cavities without any prerequisite strain and possibly increase their rate of propagation.

CONCLUDING REMARKS

A radiation environment simply represents another service condition to which engineering metals and alloys may be exposed. Structural and compositional changes induced by irradiation compound and confound alterations arising from thermal effects. This results in two distinct ductility problems: first, at low irradiation temperatures displacement damage or disruption of the crystal lattice interferes with the movement of dislocations and the development of normal deformation patterns; and, second, at high irradiation temperatures precipitation of inert gas bubbles leads to rapid nucleation and propagation of grain-boundary cracks. We cannot formulate the problem in quantitative terms, for the radiation-induced changes depend strongly on the initial structure and composition of the alloy. However, we have tried to illustrate the latitude of the problem through the behavior of type 304 stainless steel, a widely used reactor alloy.

Although we have dwelt on the problem of radiation-enhanced embrittlement, we do not mean to imply that it is an insoluble problem. In fact, a number of proposals (49,58) for overcoming the high-

temperature problem have been made, based on the mechanism of embrittlement discussed here. As such it is a good example of a case in which the solution to a problem posed by our technology arises from an understanding of the physical principles underlying the problem.

ACKNOWLEDGMENTS

We are happy to acknowledge the assistance of several members of the Metals and Ceramics Division in the preparation of this material: C.K.H. DuBose for the electron micrographs; E. E. Bloom for providing the specimens for electron microscopy and for many helpful discussions of the mechanisms of fracture; M. R. Hill for preparation of the manuscript; and K. Farrell and C. J. McHargue for technical review of the manuscript.

REFERENCES

1. M. S. Wechsler, Interaction of Radiation with Solids, ed. by R. Strumane, J. Nihoul, R. Gevers, and A. Armelinckx, North Holland Publishing Company, Amsterdam, 1965, p. 296.
2. L. E. Steele and J. R. Hawthorne, Flow and Fracture of Metals and Alloys in Nuclear Environments Spec. Tech. Publ. No. 380, American Society for Testing and Materials, Philadelphia, Pa., 1965, p. 283.
3. E. W. Hart, Theory of the Tensile Test, Acta Met. 15, 351 (February 1967).
4. C. Zener, Elasticity and Anelasticity of Metals, University of Chicago Press, Chicago, 1948, p. 158.
5. D. McLean, A Note on the Metallography of Cracking During Creep, J. Inst. Metals 85, 468 (1956-57).
6. R. C. Gifkins, A Mechanism for the Formation of Intergranular Cracks when Boundary Sliding Occurs, Acta Met. 4, 98 (1956).
7. D. Hull and D. E. Rimmer, The Growth of Grain Boundary Voids Under Stress, Phil. Mag. 4, 673 (1959).
8. A. N. Cottrell, Intercrystalline Creep Fractures, Structural Processes in Creep, Spec. Rept. No. 70, The Iron and Steel Institute, London, 1961, p. 1.
9. G. H. Kinchin and R. S. Pease, The Displacement of Atoms in Solids by Radiation, Rept. Progr. Phys. 18, 1 (1955).
10. J. B. Gibson, A. N. Goland, M. Milgram, and G. H. Vineyard, The Dynamics of Radiation Damage, Phys. Rev. 120, 1229 (1961).

11. J. R. Beeler, Jr., and D. G. Besco, Knock-on Cascades and Point Defect Configurations in Binary Materials, Radiation Damage in Solids, Symposium held in Venice, May 7-11, 1962, International Atomic Energy Agency, Vienna, 1962, p. 44.
12. J. Moteff, Radiation Damage in Body-Centered Cubic Metals and Alloys, paper presented at AIME Symposium on Radiation Effects, Asheville, N. C., September 1965, to be published in proceedings.
13. H. Alter and C. E. Weber, The Production of Hydrogen and Helium in Metals During Reactor Irradiation, J. Nucl. Mater. 16, 68 (1965).
14. J. Silcox and P. B. Hirsch, Dislocation Loops in Neutron Irradiated Copper, Phil. Mag. 4, 1356 (1959).
15. M. Wilkens and M. Ruhle, Observations of Point Defect Agglomerations in Copper by Means of Electron Microscopy, The Nature of Small Defect Clusters Consultants Symposium, Harwell, July 4-6, 1966, AERE-R 5269, p. 365.
16. M. Ruhle, Elektronenmikroskopie kleiner fehlerstellenagglomerate in bestrahlten metallen, Phys. Status Solidi 19, 279 (1967).
17. K. G. McIntyre and L. M. Brown, Diffraction Contrast from Small Defect Clusters in Irradiated Copper, The Nature of Small Defect Clusters Consultants Symposium, Harwell, July 4-6, 1966, AERE-R 5269, p. 351.
18. K. G. McIntyre, Interstitial Loops in Neutron Irradiated Copper, Phil. Mag. 15, 205 (1967).

19. M. J. Makin, F. J. Minter, and S. A. Manthorpe, The Correlation Between Critical Resolved Shear Stress of Neutron Irradiated Copper Single Crystals and the Density of Defect Clusters, *Phil. Mag.* 13, 729 (1966).
20. G. P. Scheidler, M. J. Making, F. J. Minter, and W. F. Schilling, The Effect of Irradiation Temperature on the Formation of Clusters in Neutron Irradiated Copper, The Nature of Small Defect Clusters Consultants Symposium, Harwell, July 4-6, 1966, AERE-R 5269, p. 405.
21. K. L. Merkle, Radiation Induced Point Defect Clusters in Copper and Gold, *Phys. Status Solidi* 18, 173 (1966).
22. K. L. Merkle, Radiation Induced Point Defect Clusters in Copper and Gold, The Nature of Small Defect Clusters Consultants Symposium, Harwell, July 4-6, 1966, AERE-R 5269, p. 8.
23. L. M. Howe, J. F. McGurn, and R. W. Gilbert, Direct Observation of Radiation Damage Produced in Copper, Gold, and Aluminum during Ion Bombardments at Low Temperatures in the Electron Microscope, *Acta Met.* 14, 801 (1966).
24. T. J. Koppenaar, Strength-Annealing Studies in Neutron Irradiated Copper Base Alloy Single Crystals, *Phil. Mag.* 10, 651 (1964).
25. T. J. Koppenaar, W.C.T. Yeh, and R.M.J. Cotterill, Lattice Defects in Neutron Irradiated Cu Solid Solutions, *Phil. Mag.* 12, 867 (1965).
26. B. Mastel and J. L. Brimhall, The Combined Effect of Carbon and Neutron Irradiation on Molybdenum, *Acta Met.* 13, 1109 (1965).

27. Joseph S. Bryner, The Formation of Radiation Defect Clusters in Iron During Post-Irradiation Heating, The Nature of Small Defect Clusters Consultants Symposium, Harwell, July 4-6, 1966, AERE-R 5269, p. 468.

28. B. L. Eyre and M. E. Downey, The Influence of Irradiation Temperature on the Damage Structure in Neutron Irradiated Molybdenum, The Nature of Small Defect Clusters Consultants Symposium, Harwell, July 4-6, 1966, AERE-R 5269, p. 384.

29. J. Diehl, discussion, The Nature of Small Defect Clusters Consultants Symposium, Harwell, July 4-6, 1966, AERE-R 5269, p. 570.

30. H.G.F. Wilsdorf and D. Kuhlmann-Wilsdorf, Dislocation Behavior in Quenched and Neutron Irradiated Stainless Steel, J. Nucl. Mater. 5, 178 (1962).

31. J. S. Armijo, J. R. Low, Jr., and V. E. Wolff, Radiation Effects on the Mechanical Properties and Microstructure of Type 304 Stainless Steel, USAEC Report APED-4542, General Electric Company, Vallecitos Atomic Laboratory, April 13, 1964.

32. E. E. Bloom, W. R. Martin, J. O. Stiegler, and J. R. Weir, The Effect of Irradiation Temperature on the Strength and Microstructure of Stainless Steel, J. Nucl. Mater. 22, 68 (1967).

33. D. R. Arkell and P.C.L. Pfeil, Transmission Electron Microscopical Examination of Irradiated Austenitic Steel Tensile Specimens, J. Nucl. Mater. 12, 145 (1964).

34. A. F. Rowcliffe, G.J.C. Carpenter, H. F. Merrick, and R. B. Nicholson, An Electron Microscope Investigation of the High Temperature Embrittlement of Irradiated Stainless Steels, Spec. Tech. Publ. No. 426, American Society for Testing and Materials, Philadelphia, Pa., to be published.

35. M. C. Wittels, J. O. Stiegler, and F. A. Sherrill, An Investigation of Transmutation Effects in Crystalline Solids, Phys. Status Solidi 4, 533 (1964).

36. J. Moteff, F. C. Kingsbury, and M. Hock, Influence of Dilute Rhenium Concentrations as a Result of Neutron Irradiation on the Creep Rupture Properties of Polycrystalline Tungsten, Abstract, Bulletin of the Institute of Metals Division AIME 2, 13 (1967).

37. C. Cawthorne and E. J. Fulton, The Influence of Irradiation Temperature on the Defect Structure in Stainless Steel, The Nature of Small Defect Clusters Consultants Symposium, Harwell, July 4-6, 1966, AERE-R 5269, p. 446.

38. B. Ralph, M. A. Fortes, and K. M. Bowkett, Direct Observation of Small Defect Clusters in Irradiated Metals by Field Ion Microscopy, The Nature of Small Defect Clusters Consultants Symposium, Harwell, July 4-6, 1966, AERE-R 5269, p. 395.

39. J. Diehl and D. Ast, Annealing of Vacancy Agglomerates Responsible for the Enhancement of the Critical Shear Stress of Neutron Irradiated Nickel, The Nature of Small Defect Clusters Consultants Symposium, Harwell, July 4-6, 1966, AERE-R 5269, p. 491.

40. I. G. Greenfield and H.G.F. Wilsdorf, Effect of Neutron Irradiation on the Plastic Deformation of Copper Single Crystals, *J. Appl. Phys.* 32, 827 (1961).
41. B. Mastel, H. E. Kissinger, J. J. Laidler, and T. K. Bierlein, Dislocation Channeling in Neutron Irradiated Molybdenum, *J. Appl. Phys.* 34, 3637 (1963).
42. J. L. Brimhall, The Effect of Neutron Irradiation on Slip Lines in Molybdenum, *Trans. Met. Soc. AIME* 233, 1737 (1965).
43. J. V. Sharp, Deformation of Neutron Irradiated Copper Single Crystals, *Phil. Mag.* 16, 77 (1967).
44. A. Seeger, On the Theory of Radiation Damage and Radiation Hardening, *Proc. U.N. Intern. Conf. Peaceful Uses At. Energy*, 2nd, Geneva, 1958 6, 250 (1958).
45. M. J. Makin and J. V. Sharp, A Model of "Lattice Hardening" in Irradiated Copper Crystals with the External Characteristics of "Source" Hardening, *Phys. Status Solidi* 9, 109 (1965).
46. W. R. Martin and J. R. Weir, Effect of Irradiation Temperature on the Post-Irradiation Stress-Strain Behavior of Stainless Steel, Flow and Fracture of Metals and Alloys in Nuclear Environments *Spec. Tech. Publ. No. 380*, American Society for Testing and Materials, Philadelphia, Pa., 1965, p. 251.
47. J. C. Tobin, M. S. Wechsler, and A. D. Rossin, Radiation Induced Changes in the Properties of Non-Fuel Reactor Materials, *Proc. Intern. Conf. Peaceful Uses At. Energy: 3rd, Geneva, 1964* 9, 23 (1965).

48. W. E. Murr, F. R. Shober, R. Lieberman, and R. F. Dickerson, Effects of Large Neutron Doses and Elevated Temperature on Type 347 Stainless, BMI-1609, Battelle Memorial Institute, Jan. 21, 1963; also appears as F. R. Shober and W. E. Murr, Radiation-Induced Property Changes in AISI Type 347 Stainless, Symposium on Radiation Effects on Metals and Neutron Dosimetry Spec. Tech. Publ. No. 341, American Society for Testing and Materials, Philadelphia, Pa., 1963, p. 325.
49. D. R. Harries, Neutron Irradiation Embrittlement of Austenitic Stainless Steels and Nickel Base Alloys, J. Brit. Nucl. Energy Soc. 5, 74 (1966).
50. W. R. Martin and J. R. Weir, Postirradiation Creep and Stress Rupture of Hastelloy N, Nucl. Appl. 3, 167 (March 1967).
51. A. C. Roberts and D. R. Harries, Elevated Temperature Embrittlement Induced in a 20 per cent Chromium: 25 per cent Nickel: Niobium Stabilized Austenitic Steel by Irradiation with Thermal Neutrons, Nature 200, 772 (1963).
52. W. R. Martin, J. R. Weir, R. E. McDonald, and J. C. Franklin, Irradiation Embrittlement of Low-Boron Type 304 Stainless Steel, Nature 208, 73 (1965).
53. P.R.B. Higgins and A. C. Roberts, Reduction in Ductility of Austenitic Stainless Steel after Irradiation, Nature 206, 1249 (1965).
54. D. E. Rimmer and A. H. Cottrell, The Solution of Inert Gas Atoms in Metals, Phil. Mag. 2, 1345 (1957).
55. A. H. Cottrell, Effects of Neutron Irradiation on Metals and Alloys, Met. Revs. 1, 479 (1956).

56. R. S. Barnes, Embrittlement of Stainless Steels and Nickel-Based Alloys at High Temperature Induced by Neutron Irradiation, *Nature* 206, 1307 (1965).

57. E. D. Hyam and G. Sumner, Irradiation Damage to Beryllium, Symposium held in Venice May 7-11, 1962, International Atomic Energy Agency, Vienna, 1962, p. 321.

58. W. R. Martin and J. R. Weir, Solutions to the Problems of High-Temperature Irradiation Embrittlement, Spec. Tech. Publ. No. 426, American Society for Testing and Materials, Philadelphia, Pa., to be published.

INTERNAL DISTRIBUTION

- | | | | |
|--------|-------------------------------|----------|--------------------|
| 1-3. | Central Research Library | 99. | H. Inouye |
| 4-5. | ORNL - Y-12 Technical Library | 100. | G. W. Keilholtz |
| | Document Reference Section | 101. | B. C. Kelley |
| 6-55. | Laboratory Records Department | 102. | J. A. Lane |
| 56. | Laboratory Records, ORNL R.C. | 103. | A. P. Litman |
| 57. | ORNL Patent Office | 104. | A. L. Lotts |
| 58. | G. M. Adamson, Jr. | 105. | R. N. Lyon |
| 59. | J. H. Barrett | 106. | H. G. MacPherson |
| 60. | S. E. Beall | 107. | R. E. MacPherson |
| 61. | R. J. Beaver | 108. | M. M. Martin |
| 62. | M. Bender | 109. | W. R. Martin |
| 63. | R. G. Berggren | 110. | R. W. McClung |
| 64. | J. O. Betterton, Jr. | 111. | H. E. McCoy, Jr. |
| 65. | D. S. Billington | 112. | H. C. McCurdy |
| 66. | A. L. Boch | 113. | R. E. McDonald |
| 67. | B. S. Borie | 114. | D. L. McElroy |
| 68. | G. E. Boyd | 115. | C. J. McHargue |
| 69. | W. H. Bridges | 116. | F. R. McQuilkin |
| 70. | R. B. Briggs | 117. | A. J. Miller |
| 71. | W. E. Brundage | 118. | E. C. Miller |
| 72. | D. A. Canonico | 119. | J. G. Morgan |
| 73. | R. M. Carroll | 120. | F. H. Neill |
| 74. | J. V. Cathcart | 121. | T. A. Nolan (K-25) |
| 75. | G. W. Clark | 122. | S. M. Ohr |
| 76. | K. V. Cook | 123. | P. Patriarca |
| 77. | G. L. Copeland | 124. | A. M. Perry |
| 78. | J. H. Crawford | 125. | S. Peterson |
| 79. | F. L. Culler | 126. | R. E. Reed |
| 80. | J. E. Cunningham | 127. | P. L. Rittenhouse |
| 81. | J. H. DeVan | 128. | W. C. Robinson |
| 82. | C. V. Dodd | 129. | M. W. Rosenthal |
| 83. | K. Farrell | 130. | G. Samuels |
| 84. | J. I. Federer | 131. | A. W. Savolainen |
| 85. | B. E. Foster | 132. | J. L. Scott |
| 86. | A. P. Fraas | 133. | O. Sisman |
| 87. | J. H. Frye, Jr. | 134. | G. M. Slaughter |
| 88. | R. J. Gray | 135. | S. D. Snyder |
| 89. | W. R. Grimes | 136. | I. Spiewak |
| 90. | H. D. Guberman | 137. | J. T. Stanley |
| 91. | D. G. Harman | 138. | W. J. Stelzman |
| 92. | W. O. Harms | 139-148. | J. O. Stiegler |
| 93-94. | M. R. Hill | 149. | D. Sundberg |
| 95. | N. E. Hinkle | 150. | D. B. Trauger |
| 96. | D. O. Hobson | 151. | R. P. Tucker |
| 97. | H. W. Hoffman | 152. | J. T. Venard |
| 98. | W. R. Huntley | 153. | G. M. Watson |

- | | | | |
|----------|-------------------|------|------------------|
| 154. | A. M. Weinberg | 168. | J. M. Williams |
| 155-164. | J. R. Weir, Jr. | 169. | R. O. Williams |
| 165. | W. J. Werner | 170. | J. C. Wilson |
| 166. | H. L. Whaley, Jr. | 171. | F. W. Young, Jr. |
| 167. | G. D. Whitman | 172. | C. S. Yust |

EXTERNAL DISTRIBUTION

173. C. M. Adams, Massachusetts Institute of Technology
 174-177. F. W. Albaugh, Battelle, PNL
 178-180. R. J. Allio, Westinghouse Atomic Power Division
 181. R. D. Baker, Los Alamos Scientific Laboratory
 182. C. Baroch, Babcock and Wilcox Company
 183. J. R. Beeler, North Carolina State University
 184. A. L. Bement, BMI, Pacific Northwest Laboratory
 185. L. Brewer, University of California, Berkeley
 186. V. P. Calkins, GE, NMPO
 187. S. Christopher, Combustion Engineering, Inc.
 188. T. T. Claudson, BMI, Pacific Northwest Laboratories, Richland
 189. D. B. Coburn, General Atomic
 190. F. A. Comprelli, G. E., Advanced Products Operation, San Jose, California
 191. D. F. Cope, RDT, SSR, AEC, Oak Ridge National Laboratory
 192. G. K. Dicker, Division of Reactor Development and Technology, AEC, Washington
 193. D. E. Erb, Division of Reactor Development and Technology, AEC, Washington
 194. E. A. Evans, GE, Vallecitos
 195. W. C. Francis, Idaho Nuclear Corporation
 196. A. J. Goodjohn, General Atomic
 197. R. G. Grove, Mound Laboratory
 198. D. H. Gurinsky, BNL
 199. A. N. Holden, GE, APED
 200. J. E. Irvin, BMI, Pacific Northwest Laboratory
 201-203. J. S. Kane, Lawrence Radiation Laboratory, Livermore
 204. H. Kato, U.S. Department of the Interior, Bureau of Mines
 205. E. A. Kintner, Fuel Fabrication Branch, AEC, Washington
 206. J. H. Kittel, ANL
 207. E. J. Kreih, Westinghouse, Bettis Atomic Power Laboratory
 208. W. J. Larkin, AEC, Oak Ridge Operations
 209. W. L. Larsen, Iowa State University, Ames Laboratory
 210. C. F. Leitten, Jr., Flame Plating Department, Linde Division, Union Carbide Corporation, Indianapolis
 211. P. J. Levine, Westinghouse Advanced Reactor Division, Waltz Mill Site, Box 158, Madison, Pa. 15663
 212. J. J. Lombardo, NASA, Lewis Research Center
 213. J. H. MacMillan, Babcock and Wilcox Company
 214. R. Mayfield, ANL
 215. M. McGurty, GE, NMPO

- 216. J. M. Menta, Crucible Steel Company, Hunter Research Laboratories,
P.O. Box 988, Pittsburgh, Pa.
- 217. J. Moteff, GE, Nuclear Materials and Propulsion Operation,
Cincinnati, Ohio
- 218. M. Nevitt, ANL
- 219. R. E. Pahler, Division of Reactor Development and Technology,
AEC, Washington
- 220. S. Paprocki, BMI
- 221. D. Ragone, General Atomic
- 222. W. E. Ray, Westinghouse Advanced Reactor Division, Waltz Mill
Site, Box 158, Madison, Pa., 15663
- 223. W.L.R. Rice, AGMR, AEC, Washington
- 224. B. Rubin, Lawrence Radiation Laboratory, Livermore
- 225. F. C. Schwenk, Division of Reactor Development and Technology,
AEC, Washington
- 226-228. J. M. Simmons, Division of Reactor Development and Technology,
AEC, Washington
- 229. L. E. Steele, Naval Research Laboratory
- 230. R. H. Steele, Division of Reactor Development and Technology,
AEC, Washington
- 231. W. F. Sheely, Division of Research, AEC, Washington
- 232. A. Strasser, United Nuclear Corporation
- 233. A. Taboada, Division of Reactor Development and Technology,
AEC, Washington
- 234. A. Van Echo, Division of Reactor Development and Technology,
AEC, Washington
- 235. R. Van Tyne, Illinois Institute of Technology Research Institute
- 236. C. E. Weber, Atomics International
- 237. J. F. Weissenberger, RDT, OSR, GE, NMPO
- 238. G. W. Wensch, Division of Reactor Development and Technology,
AEC, Washington
- 239. G. A. Whitlow, Westinghouse Advanced Reactor Division, Waltz Mill
Site, Box 158, Madison, Pa. 15663
- 240. E. A. Wright, AEC, Washington
- 241. Laboratory and University Division, AEC, Oak Ridge Operations
- 242-256. Division of Technical Information Extension

